Planarized Star-Shaped Oligothiophenes as a New Class of Organic Semiconductors for Heterojunction Solar Cells

ARTICLE *in* ADVANCED MATERIALS · NOVEMBER 2003

Impact Factor: 17.49 · DOI: 10.1002/adma.200305168

[1] M. Fujita, *Chem. Soc. Rev.* **1998**, *27*, 417.
[2] P. J. Stang, B. Olenyuk, *Acc. Chem. Res.* **1997**, *30*, 502.
[3] B. J. Holliday, C. A. Mirkin, *Angew. Chem. Int. Ed.* **2001**, *40*, 2022.
[4] P. H. Dinolfo, J. T. Hupp, *Chem. Mater.* **2001**, *13*, 3113.
[5] M. Yoshizawa, Y. Takeyama, T. Kusukawa, M. Fujita, *Angew. Chem. Int. Ed.* **2002**, *41*, 1347.
[6] M. Yoshizawa, Y. Takeyama, T. Okano, M. Fujita, *J. Am. Chem. Soc.* **2003**, *125*, 3243.
[7] M. L. Merlau, M. D. P. Mejia, S. T. Nguyen, J. T. Hupp, *Angew. Chem. Int. Ed.* **2001**, *40*, 4239.
[8] S.-S. Sun, A. J. Lees, *J. Am. Chem. Soc.* **2000**, *122*, 8956.
[9] M. E. Williams, K. D. Benkstein, C. Abel, P. H. Dinolfo, J. T. Hupp, *Proc. Natl. Acad. Sci. USA* **2002**, *99*, 5171.
[10] K. F. Czaplewski, J. T. Hupp, R. Q. Snurr, *Adv. Mater.* **2001**, *13*, 1895.
[11] K. F. Czaplewski, J. Li, J. T. Hupp, R. Q. Snurr, *J. Membr. Sci.* **2003**, *221*, 103.
[12] C. C. Wamser, R. R. Bard, V. Senthilathipan, V. C. Anderson, J. A. Yates, H. K. Lonsdale, G. W. Rayfield, D. T. Friesen, D. A. Lorenz, *J. Am. Chem. Soc.* **1989**, *111*, 8485.
[13] R. B. Beswick, C. W. Pitt, *Chem. Phys. Lett.* **1988**, *143*, 589.
[14] J. Zhang, M. E. Williams, M. H. Keefe, G. A. Morris, S. T. Nguyen, J. T. Hupp, *Electrochem. Solid-State Lett.* **2002**, *5*, E25.
[15] S. M. Lecours, S. G. Dimagno, M. J. Therien, *J. Am. Chem. Soc.* **1996**, *118*, 11 854.
[16] D. Hudson, *J. Org. Chem.* **1988**, *53*, 617.
[17] M. H. Keefe, *Ph.D. Thesis*, Northwestern University **2001**.
[18] W. H. Otto, M. H. Keefe, K. E. Splan, J. T. Hupp, C. K. Larive, *Inorg. Chem.* **2002**, *41*, 6172.
[19] B. Olenyuk, M. D. Levin, J. A. Whiteford, J. E. Shield, P. J. Stang, *J. Am. Chem. Soc.* **1999**, *121*, 10 434.

Planarized Star-Shaped Oligothiophenes as a New Class of Organic Semiconductors for Heterojunction Solar Cells**

By *Rémi de Bettignies*, *Yohann Nicolas*, *Philippe Blanchard*, *Eric Levillain*, *Jean-Michel Nunzi*, and *Jean Roncali**

Photovoltaic (PV) cells based on organic semiconductors are a focus of increasing research effort motivated by the possibility to realize large area, light-weight, and low-cost flexible solar cells, taking advantage of the processability of organic materials.[1–11]

Besides environmental constraints and the predictable exhaustion of fossil energy resources, the strong renewal of interest for organic PV conversion has been boosted by the large improvement in conversion efficiency of organic solar cells accomplished in recent years.[1–11]

It is widely accepted that p–n-like heterojunctions based on adequate combinations of donor (p-type) and acceptor (n-type) molecular or polymeric organic semiconductors represent the most appropriate system to achieve high power conversion efficiencies.[1–3]

[*] Dr. J. Roncali, Y. Nicolas, Dr. P. Blanchard, Dr. E. Levillain
Groupe Systèmes Conjugués Linéaires, IMMO, UMR CNRS 6501
Université d'Angers
2 Bd Lavoisier, F-49045 Angers (France)
E-mail: jean.roncali@univ-angers.fr
Dr. R. de Bettignies, Prof. J.-M. Nunzi
Cellules Photovoltaïques Plastiques, ERT 15
Université d'Angers,
2 Bd Lavoisier, F-49045 Angers (France)

[**] The authors thank TOTAL company for financial support.

Although large area heterojunctions based on interpenetrated networks of donor and acceptor molecules and/or π-conjugated polymers have reached high power conversion efficiencies,[2,4,5] significant progress has also been accomplished in organic PV cells based on vacuum evaporated or laminated multi-layer heterojunctions.[1,3,7,11] Thus, conversion efficiencies exceeding 1 % have been reported for solar cells based on phthalocyanines and acceptors derived from perylene or fullerenes C_{60}.[1,3,7,11]

Whereas thiophene-based π-conjugated oligomers have been widely investigated as organic semiconductors for application in organic field-effect transistors (OFETs),[12] their possible use in solar cells has attracted less attention.[13,14]

It is well known that a vertical orientation of the π-conjugated chains on the surface of the substrate favors high hole mobility in the corresponding OFETs.[12] Conversely, a large absorption of the incident light required for efficient PV conversion implies that the dipole of the chromophore is perpendicular to the direction of the incident light and hence parallel to the surface of the substrate. This problem has been analyzed by Fichou and co-workers, who have shown that alignment of octithiophene molecules parallel to the surface of the substrate produces a substantial improvement in power conversion efficiency of the resulting solar cells.[13]

It is generally accepted that rigid planar structures favor the high exciton mobility needed for large internal conversion quantum yields and high current densities, as illustrated by the high efficiency of solar cells based on phthalocyanines or hexabenzocoronenes.[1,15]

In this context, we report here preliminary results on solar cells based on a new π-conjugated system in which three linear oligothiophene (nTs) chains are connected to a central planar and rigid trithienobenzene core (**1**) (see Scheme 1). Using *N*,*N*′-bistridecylperylenedicarboxyimide (**3**) as the acceptor and electron-transport layer, we have carried out a comparative analysis of the spectral response and power efficiency of two series of heterojunction solar cells in which compound **1** and the linear reference compound **2** have been used as donor and hole-transport materials.

The synthesis of compounds **1** and **2** will be published elsewhere. These compounds melt at 160 and 135 °C, respectively, and can thus be easily processed by vacuum sublimation without degradation. In fact, thermogravimetry shows that compound **1** begins to degrade only above 430 °C.

Figure 1 shows the electronic absorption spectra of compounds **1** and **2** in methylene chloride solution and as thin solid films sublimed on glass.

Comparison of the solution spectra of compounds **1** and **2** shows that the absorption maximum (λ_{max}) shifts bathochromically from 379 nm (3.27 eV) for the linear compound **2** to 405 nm (3.06 eV) for the star-shaped compound **1**. This red shift shows that the combined effects of planarization and rigidification of the central core leads to a significant enhancement of π-electron delocalization associated with a decrease of the highest occupied–lowest unoccupied molecular orbital (HOMO–LUMO) gap. This conclusion is further supported

 DOI: 10.1002/adma.200305168

ADVANCED MATERIALS

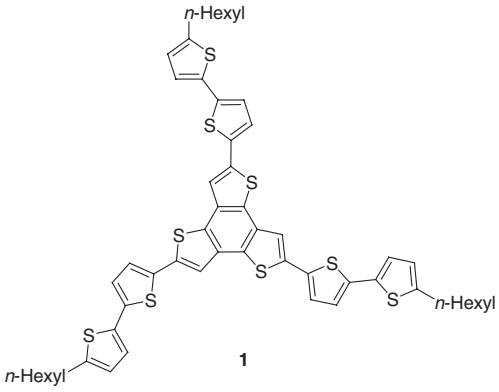

Scheme 1. Structures of compounds **1**, **2**, and **3**.

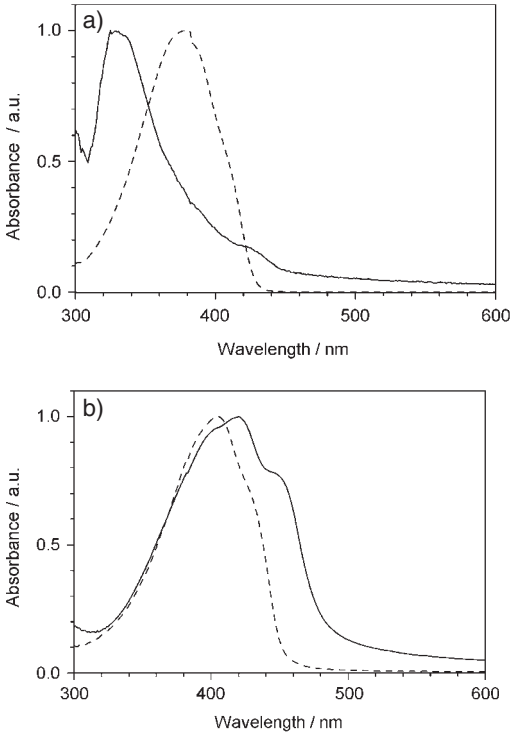

Fig. 1. Normalized electronic absorption spectra of compound **2** (a) and **1** (b). Dashed line: in methylene chloride, solid line: vacuum-sublimed thin film on glass.

by the lower oxidation potential of compound **1** (0.93 versus 1.18 V versus Ag/AgCl for **2**).[16] On the other hand, comparison of the potential shift (0.25 V) with the 0.21 eV red shift of λ_{max} shows that the decrease of the HOMO–LUMO gap from **2** to **1** results essentially from an increase of the HOMO level.

Comparison of the solution and solid-state spectra of compounds **1** and **2** reveals two very different behaviors. Thus, for compound **2**, the passage from the solution to the solid-state produces an hypsochromic shift of λ_{max} to 319 nm and the emergence of a weak new transition at 417 nm. This splitting of the singlet excited state already observed for nTs and oligothienylenevinylenes (nTVs),[12,17] has been attributed to the exciton interactions between adjacent molecules in a close-packed organization. As shown already, for both nTs and nTVs, these spectral features are associated with a vertical orientation of the molecules on the surface of the substrate.[12,13,17] In contrast, comparison of the solution and solid-state spectra of compound **1** shows that the spectrum of the solid-state film exhibits a red shift of λ_{max} from 405 to 420 nm and the emergence of a vibronic fine structure. These spectral features are strongly reminiscent of those observed on films of nTs and nTVs where the molecules are oriented parallel to the surface of the substrate.[12,13,17]

Furthermore, and although the films of both compounds have the same thickness (20 nm), the absorbance of the film of compound **1** at λ_{max} is three times larger than that of compound **2** (0.30 at 420 nm versus 0.10 at 320 nm respectively, see Fig. 2).

These considerable differences in both the shape of the spectrum and the absorption coefficient strongly suggest that, whereas molecules of the linear compound **2** adopt a vertical

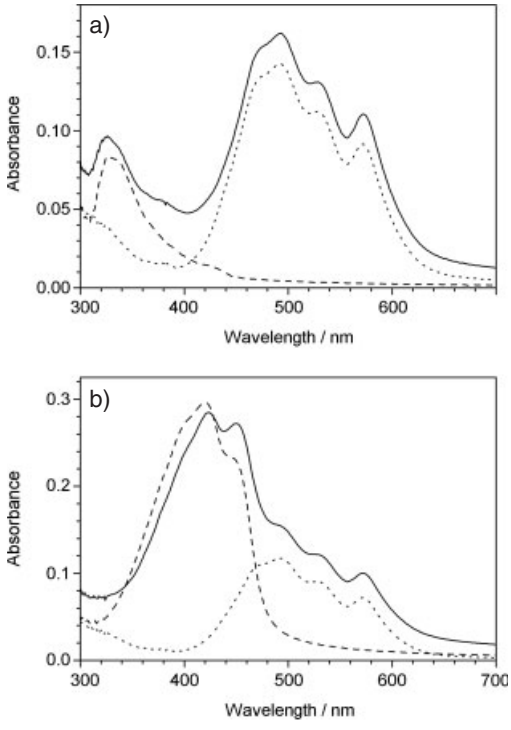

Fig. 2. Absorption spectra of the double layer of compounds **2** (a) and **1** (b) with acceptor **3.** The dotted and dashed line correspond to the individual spectra of compounds **1**, **2**, and **3** respectively (see Fig. 1).

orientation onto the surface of the substrate similarly to the parent nTs,[12,13,17] molecules of the star-shaped compound **1** adopt a preferential horizontal orientation on the indium tin oxide (ITO) surface.

This conclusion is further confirmed by the X-ray diffraction (XRD) spectra of 40 nm thick films of the two compounds. The spectrum of **2** reveals ordered layered structures (Fig. 3). From the well-resolved diffraction peaks, a diffraction spacing corresponding to a monolayer thickness of 21.4 Å has been calculated. Assuming a fully extended linear

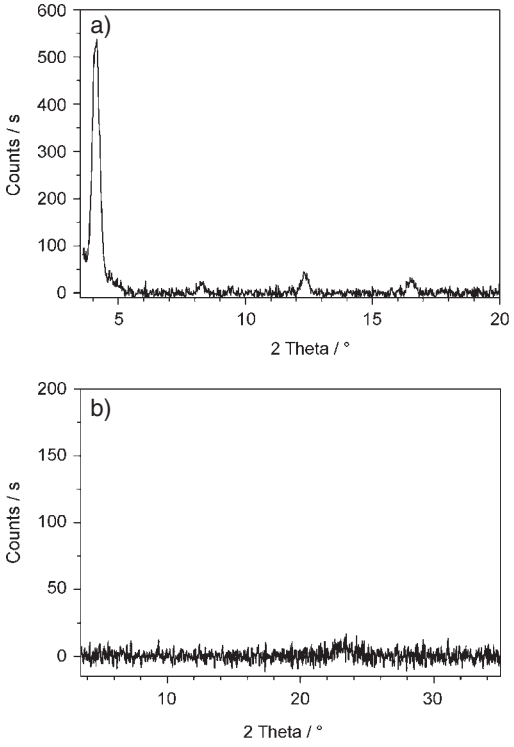

Fig. 3. XRD spectra of vacuum-evaporated films of compound **2** (a, 20 nm) and **1** (b, 40 nm); background subtracted.

structure, comparison of this result with the chain length determined using molecular models (21 Å) confirms that the molecule adopts a quasi-vertical orientation on the substrate. In contrast, the XRD spectrum of compound **1** is featureless except for a weak broad band. Although, this spectrum indicates that the film is essentially amorphous, the weak peak at $2\theta = 23.123°$ might correspond to the distance between two molecular planes (3.8 Å). However, further work is required to confirm this conclusion.

Heterojunction solar cells of 6 mm diameter have been realized on ITO substrates spin-coated with a 30 nm film of Baytron P. The donor and the acceptor layers were successively sublimed under vacuum, and the devices were completed by deposition of a 5 Å thick layer of LiF and a 80 nm thick aluminum electrode.

As shown in Figure 2, the optical spectra of the two types of solar cells are simply the sum of the spectra of the donor and acceptor. Both spectra show a broad absorption band with sub-components at 490, 530, and 580 nm, characteristic for the perylene acceptor **3**.

The photocurrent action spectrum of the two types of solar cells has been analyzed under monochromatic irradiation. The external quantum efficiency (EQE) spectrum of the cell based on donor **2** shows a maximum of 0.60 % at 480 nm which corresponds to the absorption maximum of the perylene acceptor **3**, and a value of 0.40 % at the λ_{max} of **2** (320 nm, Fig. 4). For the star-shaped donor **1**, the cell shows a much higher conversion efficiency since the EQE reaches a value of

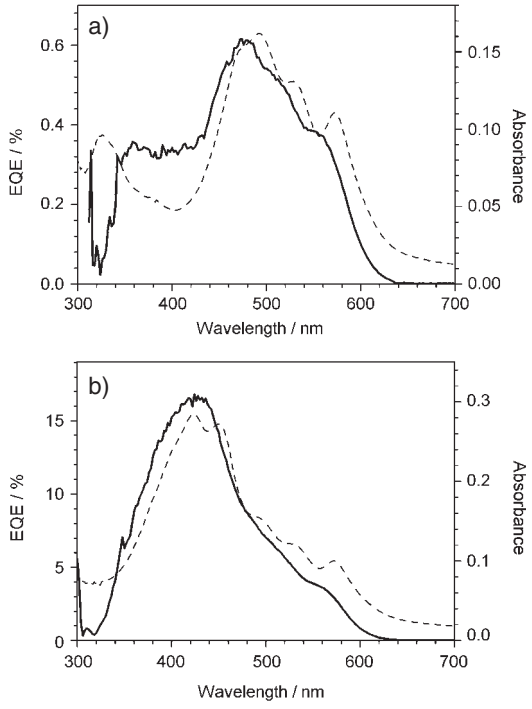

Fig. 4. Solid line—External quantum efficiency spectra (EQE) of the PV cells under monochromatic light illumination. a) donor **2**, b) donor **1**. Dotted line—absorption spectra of the cells.

17 % at λ_{max} (420 nm) and decreases then to 6–7 % in the region where absorption of the acceptor is predominant. These results clearly show that the considerable differences between the optical properties of the sublimed thin films of the two donors have important consequences for the efficiency of the corresponding solar cells.

In an attempt to optimize the performances of the cells based on the star-shaped compound **1**, the effect of the thickness of the donor layer (d) has been analyzed using a constant thickness of the acceptor layer (20 nm). Figure 5 shows the EQE spectra of three cells with $d = 13$, 20, and 40 nm. The responses clearly show that the best results are obtained with the thinnest layer. In that case, a maximum EQE of 18 % at 420 nm is obtained for $d = 13$ nm, decreasing to 17 % and 11 % for $d = 20$ and 40 nm, respectively. This decrease of EQE suggests that the efficiency is limited by the exciton diffusion length in the donor layer and that this length is at least equal to 13 nm.

ADVANCED MATERIALS

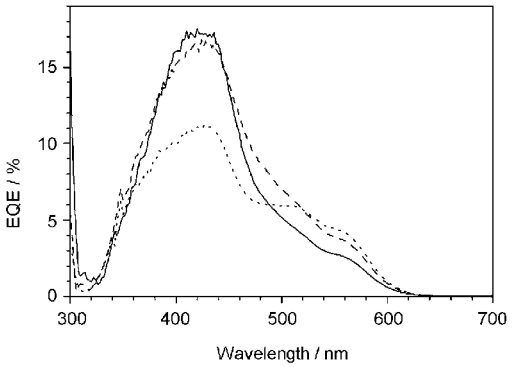

Fig. 5. Effect of the thickness (d) of the star-shaped donor **1** on the EQE spectra of the heterojunction PV cells. Solid line: $d = 13$ nm, dashed line: $d = 20$ nm, dotted line: $d = 40$ nm.

The power conversion efficiency of the various cells has been determined under white light illumination at low (1.92 mW cm^{-2}) and high (77 mW cm^{-2}) irradiation intensities. Table 1 summarizes the main photovoltaic parameters determined on the various solar cells. The cell based on the linear compound **2** shows a low rectification ratio of 31 at ±1 V in the dark. The slopes of the *I–V* curves at 0.0 and 1.0 V lead to values of 13.5 MΩ and 18.7 kΩ for the shunt (R_{sh}) and series resistance (R_s), respectively. Forward bias corresponds here to a positive voltage applied to the ITO electrode. Under low irradiation intensity (1.92 mW cm^{-2}) the device develops an open circuit voltage (V_{oc}) of 0.54 V and a short-circuit current density (J_{sc}) of 0.8 μA cm^{-2}. These values rise to 0.74 V and 94 μA cm^{-2}, respectively at 77 mW cm^{-2} irradiation intensity. In both cases, the *I–V* characteristics lead to a fill factor (FF) of 0.46, while the power conversion efficiency increases from 0.01 to 0.04 %.

Table 1. Photovoltaic parameters for the various PV cells under low (1.92 mW cm^{-2}) and high (77 mW cm^{-2}) incident power light (IPL). Thickness of the donor layer: **1a** 13 nm, **1b** 20 nm, **1c** 40 nm.

Cell	IPL [mW cm^{-2}]	V_{oc} [V]	J_{sc} [μA cm^{-2}]	FF	η [%]
1a	1.92	0.82	47.8	0.56	1.14
1a	77	0.85	1340	0.53	0.78
1b	1.92	0.78	53	0.59	1.27
1b	77	0.86	1350	0.51	0.77
1c	1.92	0.77	38.4	0.52	0.80
1c	77	0.89	969	0.51	0.57
2	1.92	0.54	0.8	0.46	0.01
2	77	0.74	94.2	0.46	0.04

Figure 6 shows the current versus voltage characteristics of the device based on the star-shaped compound **1**. The cell exhibits an excellent rectification ratio in the dark ($>10^4$ at 1.0 V) and R_{sh} and R_s values of 0.26 MΩ and 110 Ω, respectively. Under 77 mW cm^{-2} power intensity, the device gives a V_{OC} of 0.86 V and a J_{sc} of 1.35 mA cm^{-2}. FFs of 0.59 and 0.51 were determined under 1.92 and 77 mW cm^{-2} power intensity, respectively.

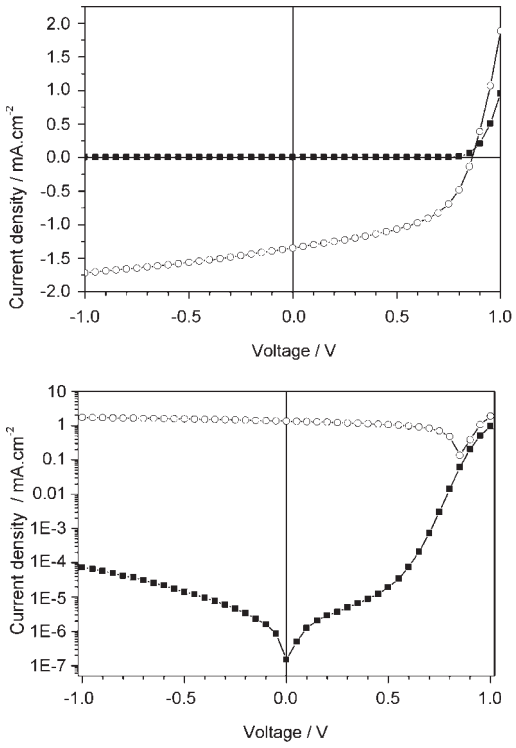

Fig. 6. Current–voltage (I–V) curves of the cell based on a 20 nm layer of donor **1** in the dark (filled squares) and under white-light illumination at 77 mW cm^{-2} (open circles).

The results obtained with the various thicknesses of the donor layer are consistent with the action spectra and show that the highest efficiencies are obtained for $d \leq 20$ nm. Under these conditions, the cells give V_{oc} higher than 0.85 V, a FF larger than 0.50, and power conversion efficiencies of ca. 0.80 %. If corrected for reflection and absorption losses at the ITO glass substrate, generally estimated to be in the range of 15–16 % in the visible region of the spectrum,[10,18] the efficiency of the cell approaches 1 %. To the best of our knowledge, these characteristics rank among the best reported so far for a solar cell based on a π-conjugated oligomer as the p-type semiconductor.

To summarize, a planarized star-shaped oligothiophene has been synthesized and used as the active material in heterojunction solar cells. Optical and XRD data for vacuum sublimed thin films are consistent with a preferential vertical orientation of the molecules onto the surface of the substrate for the linear compound, whereas molecules of the star-shaped compound seem to adopt a preferential horizontal orientation more favorable for efficient absorption of the incident light. This behavior associated with the enhanced π-electron delocalization inherent to the fused trithienobezene core lead to a considerable improvement in performance of the resulting heterojunction solar cells. These promising preliminary results thus provide a strong incitement for further research effort focused on the molecular engineering of organic semiconductors for photovoltaic solar energy conversion.

Experimental

The synthesis of compounds **1** and **2** will be published elsewhere. *N,N′*-bistridecylperylenedicarboxyimide (**3**) is commercially available (Aldrich). The ITO-coated glass substrates (Solems) with a sheet resistance of 40 Ω/□ were cleaned in an ultrasonic bath with ethanol and acetone, dried in an oven, and treated 20 min with an UV–ozone cleaner (Jelight 42–220, 28W cm^{-2}). ITO substrates were then spin-coated with a 30 nm film of poly(3,4-ethylenedioxythiophene): poly(styrenesulfonate) (PEDOT:PSS, Baytron P) and dried at 115 °C . Layers of donor and acceptor were deposited under a pressure of 5×10^{-6} mbar (Plassys ME300 chamber). Compounds **1** and **2** were deposited at a rate of 2–6 nm min^{-1}, and acceptor **3** at a rate of 10 nm min^{-1}. A glass slide placed near the ITO substrates was used to record the optical spectra of the bilayers. The devices were completed by deposition of a 0.5 nm LiF layer (rate < 2 nm min^{-1}) and a 80 nm aluminum layer (rate 20–25 nm min^{-1}) through a shadow mask with 6 mm diameter openings. All devices were then annealed 2–5 min at 90 °C. Thermal treatment and device characterizations were performed in a glove box.

Absorption spectra were recorded on a Perkin Elmer Lambda 19 UV-visible-near-IR spectrophotometer. Power conversion efficiencies were measured with a Steuernagel Solar constant 575 simulator. Light intensity was measured with a calibrated broadband optical power meter (Melles Griot) and was varied with neutral density filters.

X-ray diffraction was performed on film of 40 and 20 nm thickness for compounds **1** and **2**, respectively. Data were recorded at room temperature in reflection mode with a Philips/Enraf Nonius FR590 diffractometer using Cu Kα radiation. Ranges were 3.5° 2θ to 20° 2θ at 0.4° 2θ min^{-1} for compound **2** and 3.5° 2θ to 40° 2θ, at 0.3° 2θ min^{-1} for compound **1**.

Current versus voltage curves were recorded with a Keithley SMU 236 unit and plotted using a home made acquisition program. Illumination of the cells was done through the ITO side and the absorbance of the ITO–glass substrate was ca. 0.20 in the visible spectral region. External quantum efficiency was measured with a lock-in amplifier (Perkin Elmer 7225) under monochromatic illumination at variable wavelength at a chopping frequency of 100 Hz. The light source was a tungsten lamp (Acton SpectraPro150).

Received: March 26, 2003
Final version: July 25, 2003
Published online: September 29, 2003

[1] D. Wöhrle, D. Meissner, *Adv. Mater.* **1991**, *3*, 129.
[2] C. J. Brabec, N. S. Sariciftci, J. C. Hummelen, *Adv. Funct. Mater.* **2001**, *11*, 15.
[3] C. W. Tang, *Appl. Phys. Lett.* **1986**, *48*, 2.
[4] C. J. Brabec, G. Zerza, G. Cerullo, S. De Silvestri, S. Luzzati, J. C. Hummelen, N. S. Sariciftci, *Chem. Phys. Lett.* **2001**, *340*, 232.
[5] G. Yu, J. Gao, J. C. Hummelen, F. Wudl, A. J. Heeger, *Science* **1995**, *270*, 1789.
[6] M. Granström, K. Petritsch, A. C. Arias, A. Lux, M. R. Andersson, R. H. Friend, *Nature* **1998**, *395*, 257.
[7] a) L. S. Roman, W. Mammo, L. A. A. Pettersson, M. A. Andersson, O. Inganäs, *Adv. Mater.* **1998**, *10*, 774. b) J. Rostalski, D. Meissner, *Sol. Energy Mater. Sol. Cells* **2000**, *63*, 37.
[8] a) J. J. Dittmer, E. A. Marseglia, R. H. Friend, *Adv. Mater.* **2000**, *12*, 1270. b) K. Petritsch, J. J. Dittmer, E. A. Marseglia, R. H. Friend, A. Lux, G. G. Rozenberg, S. C. Moratti, A. B. Holmes, *Sol. Energy Mater. Sol. Cells* **2000**, *61*, 63.
[9] L. Sicot, C. Fiorini, A. Lorin, P. Raimond, C. Sentein, J.-M. Nunzi, *Sol. Energy Mater. Sol. Cells* **2000**, *63*, 49.
[10] S. A. Jenekhe, S. Yi, *Appl. Phys. Lett.* **2000**, *77*, 2635.
[11] P. Peumans, S. R. Forrest, *Appl. Phys. Lett*. **2001**, *79,* 126.
[12] a) C. D. Dimitrakopolous, P. Malenfant, *Adv. Mater.* **2002**, *14*, 99. b) H. E. Katz, A. J. Lovinger, J. G. Laquindanum, *Chem. Mater.* **1998**, *10*, 457. c) F. Garnier, A. Yassar, R. Hajlaoui, G. Horowitz, F. Deloffre, B. Servet, S. Ries, P. Alnot, *J. Am. Chem. Soc.* **1993**, *115*, 8716. d) C. Videlot, J. Ackermann, P. Blanchard, J.-M. Raimundo, P. Frère, M. Allain, R. de Bettignies, E. Levillain, J. Roncali, *Adv. Mater.* **2003**, *15*, 306.
[13] C. Videlot, A. El Kassmi, D. Fichou, *Sol. Energy Mater. Sol. Cells* **2000**, *63*, 69.
[14] N. Noma, T. Tsuzuki, Y. Shirota, *Adv. Mater.* **1995**, *7*, 647.
[15] L. Schmidt-Mende, A. Fechtenkötter, K. Müllen, E. Moons, R. H. Friend, J. D. MacKenzie, *Science* **2001**, *293*, 1119.
[16] Cyclic voltammetric measurements in 0.10 M Bu_4NPF_6–CH_2Cl_2, Pt working electrode and Ag/AgCl reference electrode, scan rate 100 mV s^{-1}.
[17] A. Yassar, G. Horowitz, P. Valat, V. Wintgens, M. Hmyene, F. Deloffrre, P. Srivastava, P. Lang, F. Garnier, *J. Phys. Chem.* **1995**, *99*, 9155.
[18] a) U. Bach, D. Lupo, P. Comte, J. E. Moser, F. Weissortel, J. Salbeck, H. Spreitzer, M. Grätzel, *Nature* **1998,** *395,* 583. b) E. Arici, N. S. Sariciftci, D. Meissner, *Adv. Funct. Mater.* **2003**, *13*, 165.

In-Situ Coating of SBA-15 with MgO: Direct Synthesis of Mesoporous Solid Bases from Strong Acidic Systems**

By *Yi Lun Wei*, *Yi Meng Wang*, *Jian Hua Zhu*,* and *Zheng Ying Wu*

Mesoporous materials are much in demand for catalysis, separation, and nanoscience, in which the well ordered hexagonal mesoporous silica SBA-15 has attracted special attention.[1] In order to broaden its application, several metals such as Al,[2] Zr,[3] Ti,[4] Ru,[5] and sulfonic[6] and phosphonic[7] acid groups have been incorporated into SBA-15 during hydrothermal synthesis. However, so far there is no report on the synthesis of basic SBA-15 directly from strong acid solution.

Mesoporous basic materials are extremely desirable for the developmet of environmentally benign chemical processes. However, their preparation methods are limited and characterized by two separate steps. Traditionally, the mesoporous host must be synthesized first, then the basic guests or their precursors are loaded through one of several processes like ion exchange, impregnation,[8] or microwave radiation,[9,10] costing energy and time and sometimes producing waste.

Here, we present the first synthesis of basic mesoporous materials directly from strong acidic solution. This is achieved by in-situ coating of SBA-15 with basic MgO by adding acetate salt into the initial mixture of raw materials for synthesis and performing both synthesis and modification in a one-step procedure to form a novel material with a mesoporous structure and strong basicity.

All synthesized MgO/SBA-15 composites exhibit the typical X-ray diffraction (XRD) patterns of the two-dimensional (2D) hexagonal pore ordering of the *p6mm* space group, identical to that of SBA-15 (Fig. 1), which indicates the existence of mesoscopic order in these mesoporous basic composites. Moreover, the intensities of the peaks of the calcined MgO/SBA-15 samples synthesized by this method are much stronger than those of the control sample, calcined SBA-15 impregnated by the traditional process. For the control sample, the intensity decreased markedly after the basic species was loaded.[10] The 77 K N_2 adsorption–desorption isotherms of MgO/SBA-15 composites shown in Figure 2A are type IV with a clear H_1-type hysteresis loop at high relative pressure. However, the desorption branch of the isotherms and the shape of the hysteresis loop show the characteristics of ink-bottle pores, signifying some degree of pore blocking that results from the coating of MgO. It is worth pointing out that the basic composites made by this method have large surface areas and pore volumes (Table 1), higher than those with the same load but prepared by impregnation (for instance, MgO/

[*] Prof. J. H. Zhu, Y. L. Wei, Y. M. Wang, Z. Y. Wu
Department of Chemistry, Nanjing University
Nanjing 210093 (China)
E-mail: jhzhu@netra.nju.edu.cn

[**] This work was supported by NSF of China (20273031), Ningbo Cigarette Factory, and Analysis Center of Nanjing University.

 DOI: 10.1002/adma.200305803